ACS Catalysis

Research Article

pubs.acs.org/acscatalysis

Role of Keto Intermediates in the Hydrodeoxygenation of Phenol over Pd on Oxophilic Supports

Priscilla M. de Souza,[†,‡] Raimundo C. Rabelo-Neto,[†] Luiz E. P. Borges,[‡] Gary Jacobs,[§] Burtron H. Davis,[§] Tawan Sooknoi,[∥] Daniel E. Resasco,[∥] and Fabio B. Noronha*[,†,‡]

[†]Catalysis Division, National Institute of Technology,, Av. Venezuela 82, Rio de Janeiro, RJ 20081-312, Brazil

[‡]Chemical Engineering Department, Military Institute of Engineering, Praça Gal. Tiburcio 80, Rio de Janeiro, RJ 22290-270, Brazil

[§]Center for Applied Energy Research, The University of Kentucky, 2540 Research Park Drive, Lexington, Kentucky 40511, United States

[∥]Center for Biomass Refining, School of Chemical, Biological, and Materials Engineering, The University of Oklahoma, , 100 East Boyd Street, Norman, Oklahoma 73019, United States

S *Supporting Information*

ABSTRACT: The performance of Pd catalysts supported on SiO_2, Al_2O_3 and ZrO_2 for the hydrodeoxygenation (HDO) of phenol has been compared in the gas phase, at 300 °C and 1 atm using a fixed bed reactor. While Pd supported on SiO_2 and Al_2O_3 exhibits high selectivity to cyclohexanone, when supported on an oxophilic support such as ZrO_2, it favors the selectivity toward benzene, reducing the formation of ring-hydrogenated products, cyclohexanone and cyclohexanol. Diffuse reflectance infrared Fourier transform spectroscopy experiments support the participation of a keto-tautomer intermediate (2,4-cyclohexadienone) in the reaction. This intermediate can be hydrogenated in two different pathways. If the ring is hydrogenated, cyclohexanone and cyclohexanol are dominant products, as in the case of Pd/SiO_2 and Pd/Al_2O_3 catalysts. By contrast, if the carbonyl group of the keto-intermediate tautomer is hydrogenated, benzene is directly formed via rapid dehydration of the unstable cyclohexadienol intermediate. This is observed in the case of Pd/ZrO_2 catalyst. These results demonstrate that the selectivity for HDO of phenol can be controlled by using supports of varying oxophilicity.

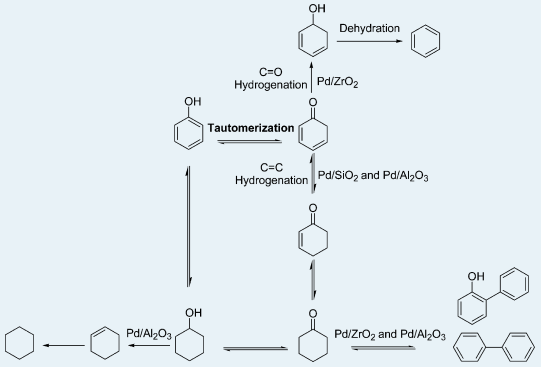

KEYWORDS: *phenol, Pd/ZrO_2, hydrodeoxygenation, biomass, bio-oil*

1. INTRODUCTION

Oxygen removal is an important step in biofuel upgrading that can be accomplished by different reaction paths such as dehydration, hydrogenation, and hydrogenolysis. Particular attention has been recently devoted to the upgrading of pyrolysis oils derived from lignocellulosic biomass. This so-called second-generation biofuel is of importance for contributing not only to energy security but also to the reduction of CO_2 emissions, without competing with food production. During the past few years, catalytic hydrodeoxygenation (HDO) has been extensively investigated for a number of bioavailable precursors derived from the conversion of hemicellulose (branched polymers of different sugar monomers) and cellulose (i.e., unbranched polymers of glucose), which are embedded in the cell walls of plants.

Researchers have particularly targeted specific model feeds such as acetic acid, glycerol, furfural, HMF, and guaiacol to represent the different families of biomass-derived compounds.[1−10] Because of high reactivity due to their O content, these compounds have often been subjected to HDO reactions to improve their stability and potential to be used as fuel components.[11−14]

Traditionally, HDO catalysts have been based on sulfided NiMo or CoMo supported on alumina.[15] With this type of catalyst, hydroprocessing conditions are rather severe (pressures on the order of hundreds of atmospheres and temperatures in the range of 673−773 K).[16] However, considering the importance of biofuel constituents as building blocks for transportation fuels, it has been recognized that novel HDO catalysts that can operate under milder conditions would be highly desirable. Moreover, different catalyst formulations might be tailored to achieve different product selectivities for specific needs. For example, it has been found that Cu/SiO_2 catalysts operating at atmospheric pressure produce furfuryl alcohol from furfural by hydrogenating the carbonyl group, whereas Pd and Ni catalysts are active for decarbonylation, yielding furan as the main product.[11] A

Received: September 19, 2014
Revised: January 10, 2015
Published: January 15, 2015

DOI: 10.1021/cs501853t
ACS Catal. 2015, 5, 1318−1329

comparison among the performance of Co, Ni, Pd, and Pt supported on SiO_2 for HDO of guaiacol in the liquid phase was carried out by Mochizuki et al.[17] Pd/SiO_2 exhibited a much higher activity than Ni-based catalysts for deoxygenation of guaiacol at 573 K and 5 MPa. More recently, Pd catalysts supported on SiO_2 and ZrO_2 have been tested for the hydrodeoxygenation (HDO) of *m*-cresol in the gas phase at 573 K and 1 atm using a fixed-bed reactor.[18] In comparison to Pd/SiO_2, the catalyst supported on ZrO_2 exhibits a dramatic enhancement in selectivity toward the deoxygenated product (toluene). It was proposed that ZrO_2 contains oxophilic sites that favor the interaction with the oxygen end of the CO group in comparison to the aromatic ring. This preference facilitates the hydrogenation of the carbonyl and leads to the formation of toluene.

Phenol is another important model compound that only exhibits a single functionality.[19−21] Several catalysts based on Ni, Co, Fe, Pt, Pd, and Ru dispersed on different supports have been studied for the HDO of phenol in the liquid or gas phase.[22−33] For example, Mortensen et al. studied the HDO of phenol in the liquid phase for Pt, Pd, and Ru supported on carbon.[34] They reported the following order of activity for deoxygenation: Ru > Pd > Pt. However, cracking reactions were observed on Ru/C catalyst. However, there has been no systematic study comparing the performance of all of these metals deposited over the same support. Mortensen et al. also investigated the performance of Ni supported on different materials (Ni/ZrO_2, $Ni\text{-}V_2O_5/ZrO_2$, $Ni\text{-}V_2O_5/SiO_2$, Ni/Al_2O_3, Ni/SiO_2, $Ni/MgAl_2O_4$, $Ni/CeO_2\text{-}ZrO_2$, Ni/CeO_2, Ni/C) for the HDO of phenol in the liquid phase.[34] They found that Ni/ZrO_2 was the most selective catalyst for the formation of cyclohexane. It was suggested that phenol is adsorbed on coordinatively unsaturated metal sites in the oxide surface (Zr cations), stabilizing the phenoxide ion that interacts with Ni, facilitating the hydrogenation of the aromatic ring and producing cyclohexanone, which rapidly produces cyclohexanol. This alcohol would later be dehydrated to cyclohexene, followed by hydrogenation to cyclohexane. In previous studies, we have questioned this mechanism, pointing out that partial hydrogenation of the aromatic ring most probably does not occur because HDO is also observed on catalysts which have little or no dehydration activity for converting a saturated alcohol such as cyclohexanol to the olefin, cyclohexene. As a result, we have proposed that a direct pathway for HDO should occur. However, C−OH bond cleavage cannot occur with an arylic C, leading to a proposed path that involves a keto tautomer intermediate.[35−38]

The goal of this work is to further compare the product distribution of HDO of phenol over Pd catalysts supported on different oxides. The analysis of reaction pathways combined with diffuse reflectance infrared Fourier transform spectroscopy (DRIFTS) measurements might shed some light on the reaction mechanism.

2. EXPERIMENTAL SECTION

2.1. Catalyst Synthesis. SiO_2 (Hi-Sil 915) and Al_2O_3 (Puralox) supports were obtained from PPG Industries Inc. and Sasol, respectively. The ZrO_2 support was synthesized by the precipitation method. A solution of 2.0 M zirconyl nitrate (35 wt % $ZrO(NO_3)_2$ in dilute nitric acid (>99%, Sigma-Aldrich) was added slowly to a solution of 4.0 M ammonium hydroxide (NH_4OH, Vetec) at room temperature and vigorously stirred for 30 min. The resulting precipitate was filtered and washed with distilled water until a pH of 7 was reached. Then, the solid was dried at 383 K for 12 h and calcined under a dry air flow at 773 K (heating ramp 5 K/min) for 6 h.

Pd/SiO_2, Pd/Al_2O_3, and Pd/ZrO_2 catalysts with a nominal Pd loading of 2.0 wt % were prepared by incipient wetness impregnation of the supports with an aqueous solution of $Pd(NO_3)_2$ (Merck). After impregnation, the powder was dried in air at 293 K for 12 h and then calcined in air at 673 K for 3 h (2 K/min). A Pd/ZrO_2 catalyst containing 1.0 wt % of Pd was also prepared using $Pd(NH_3)_4(NO_3)_2$ (Sigma-Aldrich) as a precursor salt. This sample was calcined under the same conditions as previously described. The Pd/ZrO_2 catalysts are referred to in the text as Pd/ZrO_2-N ($Pd(NO_3)_2$) and Pd/ZrO_2-T ($Pd(NH_3)_4(NO_3)_2$). Ni/SiO_2 and Ni/ZrO_2 catalysts with a nominal Ni loading of 10.0 wt % were also prepared by incipient wetness impregnation of the supports with an aqueous solution of $Ni(NO_3)_2{\cdot}H_2O$ (Merck). The samples were calcined under the same conditions as those for the Pd-based catalysts.

2.2. Catalyst Characterization. The chemical composition of each sample was determined by optical emission spectroscopy (ICP-OES). Specific surface areas of the samples were measured using a Micromeritics ASAP 2000 analyzer by N_2 adsorption at the boiling temperature of liquid nitrogen. The X-ray powder diffraction (XRD) patterns were obtained on a Rigaku diffractometer using Cu Kα radiation (λ = 1.5406 Å) over a 2θ range of 10−80° at a scan rate of 0.04°/step and a scan time of 1 s/step. The Pd dispersion was measured by CO chemisorption using the dynamic adsorption method. Before adsorption, the samples (50 mg) were reduced under pure H_2 (60 mL/min) at 573 K for 1 h (10 K/min), cooled to room temperature, and flushed in He for 30 min. Then, 1 mL pulses of 5% CO in He were injected until saturation was reached, as monitored by a quadrupole mass spectrometer (MKS Cirrus 200). The Pd dispersion was calculated assuming a stoichiometry of 1:1 for CO adsorbed on Pd.

The surface properties of the catalysts were investigated by diffuse-reflectance infrared Fourier transform spectroscopy (DRIFTS), using pyridine as a probe molecule. For each catalyst sample, prereduction was conducted in situ at 573 K for 1 h under a flow of H_2 of 30 mL/min, and then the catalyst was cooled to 373 K and exposed to pyridine vapor for approximately 30 min. The samples were then purged under a H_2 flow for 20 min. Background and absorption spectra were recorded at a resolution of 4 cm^{-1}, accumulating 256 scans in each measurement.

In order to investigate the reaction mechanism, experiments were performed in the DRIFTS in situ cell under conditions similar to those employed in the HDO reaction. DRIFTS spectra were recorded using a Nicolet Nexus 870 spectrometer equipped with a DTGS-TEC detector. A Thermo Spectra-Tech cell capable of high-pressure/high-temperature operation and fitted with ZnSe windows served as the reaction chamber for in situ adsorption and reaction measurements. Scans were taken at a resolution of 4 cm^{-1} to give a data spacing of 1.928 cm^{-1}. The number of scans taken was 512. The amount of catalyst was ~40 mg.

The sample was reduced in H_2 at 573 K for 1 h and cooled to 323 K in He, and a background spectrum was recorded. Pure H_2 was then flowed through a bubbler containing the compound of interest (phenol, 351 K; cyclohexanone, 323 K; cyclohexanol, 340 K) and the temperature was raised to 373,

DOI: 10.1021/cs501853t
ACS Catal. 2015, 5, 1318−1329

Table 1. Pd Composition, Specific Surface Area, CO Chemisorption, Pd Dispersion, and Turnover Frequency for Deoxygenation of Pd-Based Catalysts

catalyst	precursor	amt of Pd (wt %)[a]	BET (m^2/g)	CO uptake (μmol/(g of cat))	dispersion[b] (%)	TOF_{HDO} (s^{-1})
Pd/SiO_2	$Pd(NO_3)_2$	1.92	172	43.7	18.6	0.04
Pd/ZrO_2-N	$Pd(NO_3)_2$	2.24	84	101.1	39.8	0.11
Pd/ZrO_2-T	$Pd(NH_3)_4(NO_3)_2$	0.89	89	19.8	23.7	0.09
Pd/Al_2O_3	$Pd(NO_3)_2$	2.28	134	25.3	21.6	0.05

[a]Measured by ICP-OES. [b]Pd:CO stoichiometry of 1:1.

473, 573, 673, and 773 K. For TPD experiments, He was utilized as a carrier gas in lieu of H_2.

2.3. Catalytic Activity. The vapor-phase conversion of the oxygenate compound of interest (phenol, cyclohexanol, or cyclohexanone) was carried out in a fixed-bed quartz reactor, operating at atmospheric pressure of H_2 and 573 K. Prior to the reaction, the catalyst was reduced in situ under pure H_2 (60 mL/min) at 573 K for 1 h. The catalysts were diluted with inert material (m_{SiC}/m_{catal} = 3.0) to avoid hot-spot formation. The reactant mixture was obtained by flowing H_2 through the saturator containing the organic compound, which was kept at the specific temperature required to obtain the desired H_2/organic compound molar ratio (about 60). To avoid condensation, all lines were heated to 523 K. The reaction products were analyzed by an Agilent Technologies 7890A/5975C GCMS, using an HP-Innowax capillary column and a flame ionization detector (FID). Each of the catalysts investigated was evaluated at different W/F values by varying the catalyst amount in the range 2.5−120 mg. The W/F value is defined as the ratio of catalyst mass (g) to organic feed mass flow rate (g/h). The product yield and selectivity for each product were calculated as follows:

$$\text{yield (\%)} = \frac{\text{mol of product produced}}{\text{mol of phenol fed}} \times 100 \quad (1)$$

$$\text{selectivity (\%)} = \frac{\text{mol of product produced}}{\text{mol of phenol consumed}} \times 100 \quad (2)$$

The turnover frequency was calculated by using the reaction rate for the formation of deoxygenated products (benzene and cyclohexane) and the Pd dispersion as measured by CO chemisorption.

3. RESULTS AND DISCSSION

3.1. Catalyst Characterization. Table 1 summarizes the characteristics of the catalysts investigated. The CO uptake and the calculated dispersion of the catalysts containing 2 wt % Pd changed depending on the support. Pd/SiO_2 and Pd/Al_2O_3 catalysts exhibited the same metal dispersion, whereas the dispersion of Pd/ZrO_2-N was twice that of the SiO_2- and Al_2O_3-supported Pd catalysts. Therefore, to be able to make a comparison with different supports at the same dispersion, a second ZrO_2-supported catalyst (Pd/ZrO_2-T) was prepared with a Pd dispersion of 24%, which is comparable to that of the other catalysts.

X-ray diffraction patterns for Pd/SiO_2, Pd/ZrO_2-N, and Pd/Al_2O_3 catalysts are shown in Figure S1 (Supporting Information). The Pd/SiO_2 catalyst exhibited broad peaks corresponding to amorphous SiO_2 and PdO (2θ = 33.8, 54.7, 60.2, and 70.9°) (JCPDS 41-1107). The diffractogram of Pd/ZrO_2-N showed lines characteristic of a mixture of monoclinic (JCPDS 37-1484) and tetragonal ZrO_2 (JCPDS 17-0923). The nature of the ZrO_2 phase depends on the preparation method and has a direct influence on both acid/base properties and surface hydroxyl group concentrations.[39] The characteristic lines of PdO were not detected for this catalyst due to the superposition with diffraction lines of the ZrO_2 phases and the high Pd dispersion of this sample. The Pd/Al_2O_3 catalyst displayed diffraction lines associated with different phases of Al_2O_3: θ-Al_2O_3 (JCPDS 35-0121), δ-Al_2O_3 (JCPDS 46-1131), and γ-Al_2O_3 (JCPDS 10-0425).

The DRIFTS spectra of pyridine absorbed on the Pd/SiO_2, Pd/ZrO_2-N, and Pd/Al_2O_3 catalysts after evacuation at 473 K are compared in Figure 1. The spectrum of the Pd/SiO_2 catalyst does not exhibit any bands. For Pd/ZrO_2-N, two bands at 1444 and 1604 cm^{-1} and broad bands at 1488 and 1574 cm^{-1} are observed. All of these bands can be assigned to vibrational modes of pyridine coordinated to uncoordinated Zr cations.[40,41] In addition to the bands corresponding to Lewis acid sites, the DRIFTS spectrum of pyridine adsorbed on Pd/Al_2O_3 also reveals bands assigned to Brønsted acid sites (1550 cm^{-1}). These results indicate that both Brønsted and Lewis acid sites exist on the surface of the Pd/Al_2O_3 catalyst, while Pd/ZrO_2-N shows predominantly Lewis acid sites. Pd/SiO_2 does not exhibit any measurable acidity. Thus, the following order of density of acid sites is observed: Pd/Al_2O_3 > Pd/ZrO_2-N > Pd/SiO_2.

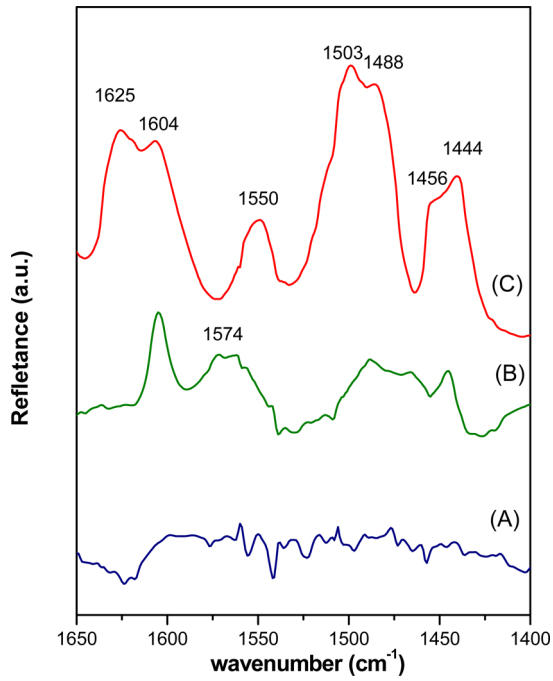

Figure 1. DRIFT spectra of adsorbed pyridine on (A) Pd/SiO_2, (B) Pd/ZrO_2-N, and (C) Pd/Al_2O_3.

DOI: 10.1021/cs501853t
ACS Catal. 2015, 5, 1318−1329

3.2. HDO of Phenol over Pd/SiO_2, Pd/ZrO_2, and Pd/Al_2O_3 Catalysts. The phenol conversion and product yield as a function of W/F at 573 K over Pd/SiO_2, Pd/ZrO_2-N, and Pd/Al_2O_3 catalysts are shown in Figure 2. It is clear that the Pd/ZrO_2-N catalyst was much more active than the Pd/SiO_2 and Pd/Al_2O_3 catalysts, which exhibited approximately the same conversion. The bare supports were also tested and were found to be inactive under the reaction conditions used. Therefore, the catalyst activity should be attributed to either the metallic function or a bifunctional metal−support interaction. To quantify the difference in specific deoxygenation rates over the catalysts, the turnover frequency (TOF) was calculated using the data obtained under differential reaction conditions (conversion around 10%), and the results are given in Table 1. The TOF over Pd/ZrO_2 catalysts was about 2 times higher than that over Pd/SiO_2 and Pd/Al_2O_3, which suggests that the ZrO_2 support enhances the deoxygenation activity.

The product distributions showed a remarkable dependence on the support used. For Pd/SiO_2 and Pd/Al_2O_3 catalysts, cyclohexanone (ONE) was the main product formed at $W/F <$ 0.4 h. Significant yields of benzene were only obtained at higher W/F. Small amounts of cyclohexanol (OL) were also observed on the Pd/SiO_2 catalyst, whereas C_{12} hydrocarbons such as biphenyl and cyclohexylbenzene were formed on Pd/Al_2O_3 catalyst. In contrast, over the Pd/ZrO_2 catalyst, benzene was the dominant product across the entire W/F range, with only small amounts of cyclohexanone (ONE) and traces of C_{12} hydrocarbons observed.

For the purpose of comparison, Table 2 summarizes the product distribution over all catalysts at similar levels of conversion (around 10%). Clearly, the product selectivities obtained on the two Pd/ZrO_2 catalysts are drastically different from those on Pd/SiO_2 and Pd/Al_2O_3 catalysts. For both zirconia-supported catalysts, the selectivity to benzene was about 3-fold higher than that on the SiO_2- or Al_2O_3-supported Pd catalysts.

The effect of Pd particle size on the product distribution can be evaluated from the results obtained on the Pd/ZrO_2-T and Pd/ZrO_2-N catalysts, which have different Pd dispersions. Both catalysts exhibited similar selectivities, indicating that metal dispersion does not significantly affect the product distribution in the HDO of phenol. Recently, a very similar result was observed for the HDO of *m*-cresol over Pd/ZrO_2 catalysts.[18]

Finally, the HDO of phenol over a physical mixture of a Pd/SiO_2 catalyst with the bare ZrO_2 support was carried out. The aim of this experiment was to determine whether the changes in selectivity were due to a direct interaction between the support and the metal or rather to the sum of separate independent functions (i.e., metal + support). The product distribution of the physical mixture was very similar to that of the Pd/SiO_2 catalyst, with a high selectivity to ONE, regardless of the presence of ZrO_2 (Table 2). This result demonstrates that the remarkable performance of the Pd/ZrO_2 catalyst for the HDO of phenol is not due to the addition of two independent phenomena but rather to an intimate contact between the metal and the ZrO_2 support. Therefore, it is conceivable that the highly selective catalysis occurs at the metal−support interface.

The electronic effect of the support has been claimed as being responsible for changes in the adsorption and catalytic properties of the metal for different reactions. This might be another alternative explanation for the highest activity for deoxygenation of Pd/ZrO_2 catalyst. If the support affects the electronic property of Pd nanoparticle, then the selectivity to deoxygenated products should change depending on the Pd dispersion. An electronic effect would be most pronounced for

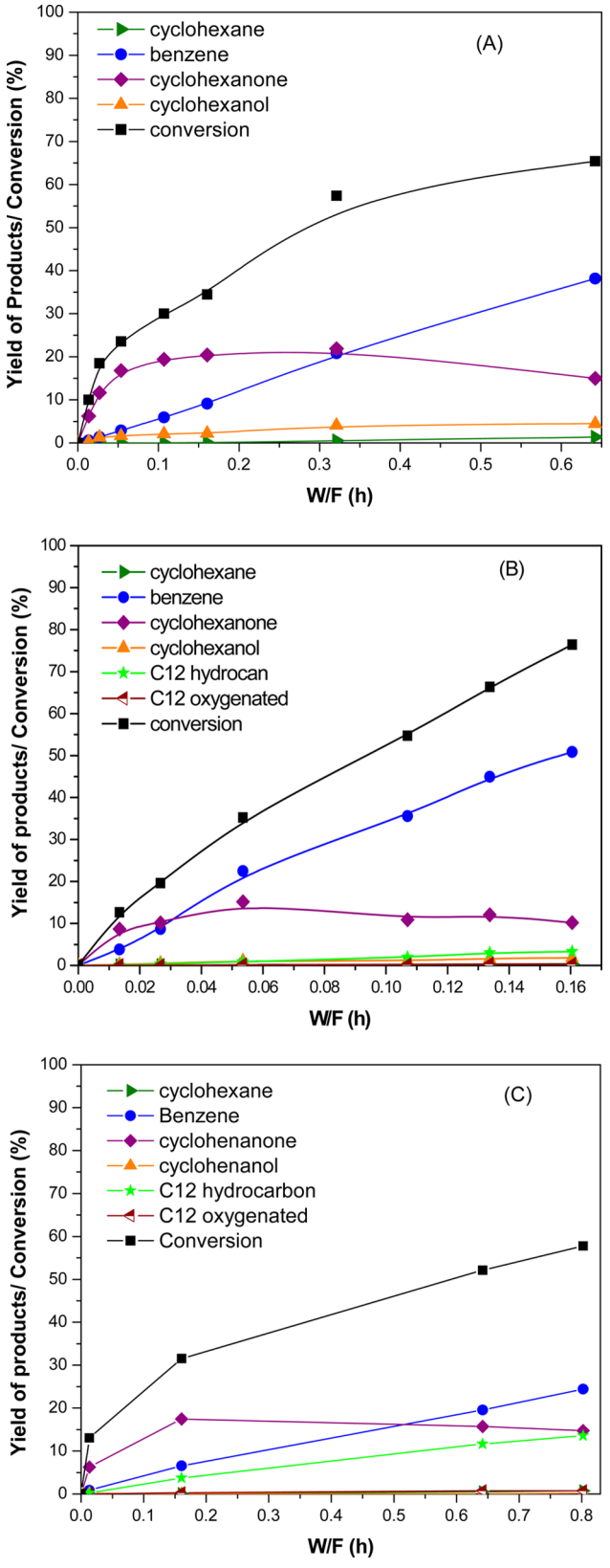

Figure 2. Phenol conversion and yield of products as a function of W/F over (A) Pd/SiO_2, (B) Pd/ZrO_2-N, and (C) Pd/Al_2O_3. Reaction conditions: T = 573 K, P = 1 atm, and H_2/phenol molar ratio 60.

DOI: 10.1021/cs501853t
ACS Catal. 2015, 5, 1318−1329

Table 2. Product Distribution for HDO of Phenol at 573 K and Atmospheric Pressure over Pd-Based Catalysts

		selectivity (%)			
	conversion (%)	benzene	ONE	OL	C_{12}
Pd/SiO_2	6.9	8.1	88.9	3.0	0.0
Pd/ZrO_2-N	12.6	29.9	68.7	1.3	0.0
Pd/ZrO_2-T	9.9	26.3	70.3	1.5	0.0
Pd/Al_2O_3	7.5	11.1	84.1	2.0	2.8
$Pd/SiO_2 + ZrO_2$	12.1	10.3	87.9	1.2	0.0

the smaller Pd particles (2.9 nm), in which more Pd atoms are in direct contact with the support, than for the larger particles (4.9 nm). When the particle size varies from 2.9 to 4.9 nm, the number of atoms in the particle increases by a factor of 3. The additional atomic layers of Pd present in the latter case would considerably weaken any electronic effect from the support. Therefore, one would expect selectivity to deoxygenated products to be significantly higher for the catalyst with higher Pd dispersion. However, the selectivities only slightly increased when the particle size decreased.

On the other hand, if the selectivity to deoxygenated products is governed by the metal−support interface, then one would expect selectivity to be less sensitive to the change in diameter with an increase in particle size from 2.9 to 4.9 nm than that of an electronic effect. This is because the number of atoms in the perimeter decreases only 1.7 times when the particle size varies from 2.9 to 4.9 nm. Thus, though we do not rule out the presence of an electronic effect from the support, the results favor an explanation involving the influence of a junction between Pd particles and defect sites in zirconia on improving benzene selectivity.

In order to further elucidate the nature of species participating in this selective path, conversion tests with intermediate products (e.g., cyclohexanol and cyclohexanone) were performed over all catalysts and supports together with DRIFTS studies under the same reaction conditions.

3.3. Cyclohexanol and Cyclohexanone Conversion over Pd/SiO_2, Pd/ZrO_2, and Pd/Al_2O_3 Catalysts. Figure 3 shows the conversion and product yields for the HDO of cyclohexanone over all catalysts. The conversion of ONE over all catalysts yielded predominantly phenol as the main product. At the same time, C_{12} hydrocarbons (biphenyl, cyclohexylbenzene) and C_{12} oxygenated compounds (2-phenylphenol, 2-cyclohexylphenol, 2-cyclohexylcyclohexan-1-one) were also produced over Pd/Al_2O_3 and Pd/ZrO_2. Likewise, the conversion and product yields for HDO of cyclohexanol over all catalysts are summarized in Figure 4. Pd/Al_2O_3 catalyst was much more active than Pd/SiO_2 and Pd/ZrO_2 catalysts. Phenol, benzene, and cyclohexanone were produced over all catalysts when OL was used as the feed. In addition, cyclohexane and cyclohexene were also formed in significant amounts over the Pd/Al_2O_3 catalyst.

Table 3 compares product yields for each feed at approximately the same conversion level. For Pd/SiO_2 and Pd/ZrO_2-N catalysts, cyclohexanol was preferentially dehydrogenated to phenol, indicating that this reaction is fast. In addition, ONE and benzene were also formed when OL was fed over the three supported Pd catalysts. The formation of significant amounts of benzene might indicate that the dehydration of the cyclohexanol reaction could take place on all supports. However, separate studies indicate that this contribution is not dominant. Indeed, to determine the extent

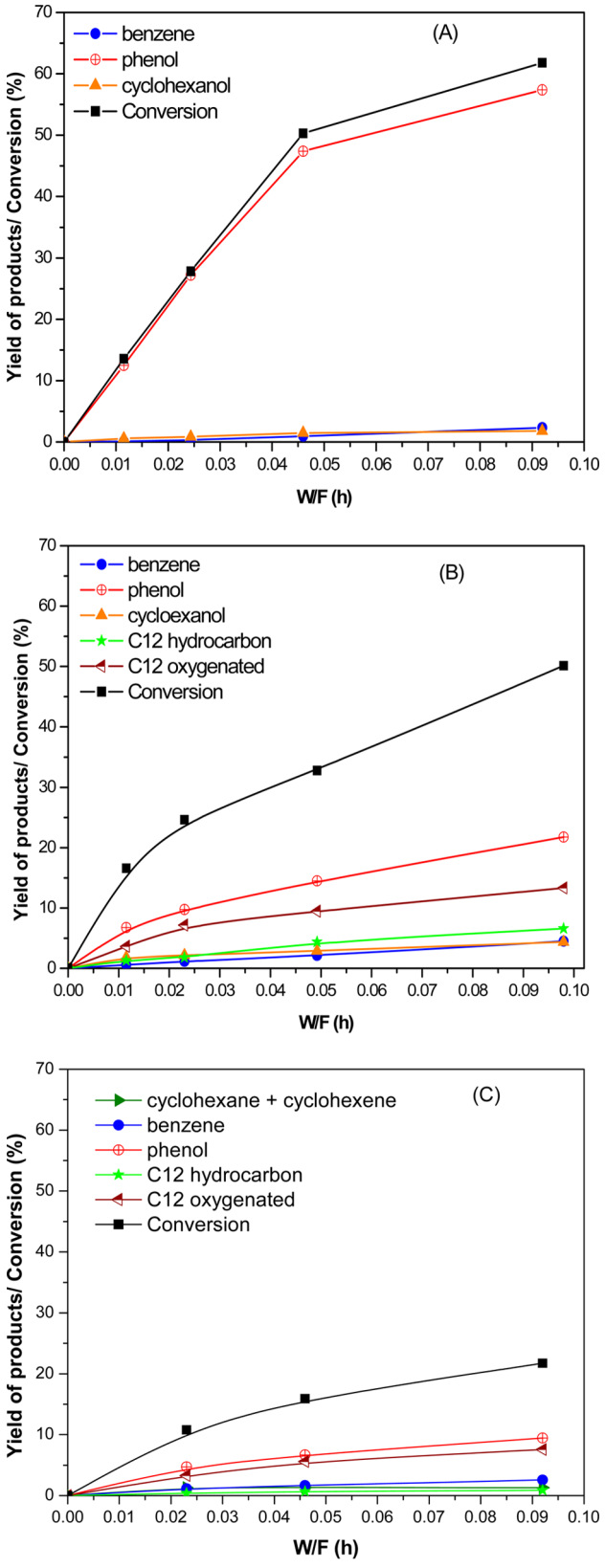

Figure 3. Cyclohexanone conversion and yield of products as a function of W/F over (A) Pd/SiO_2, (B) Pd/ZrO_2-N, and (C) Pd/Al_2O_3. Reaction conditions: T = 573 K, P = 1 atm, and H_2/cyclohexanone molar ratio 60.

of dehydration catalyzed by the support alone, cyclohexanol conversion was carried out over the pure supports at the

DOI: 10.1021/cs501853t
ACS Catal. 2015, 5, 1318−1329

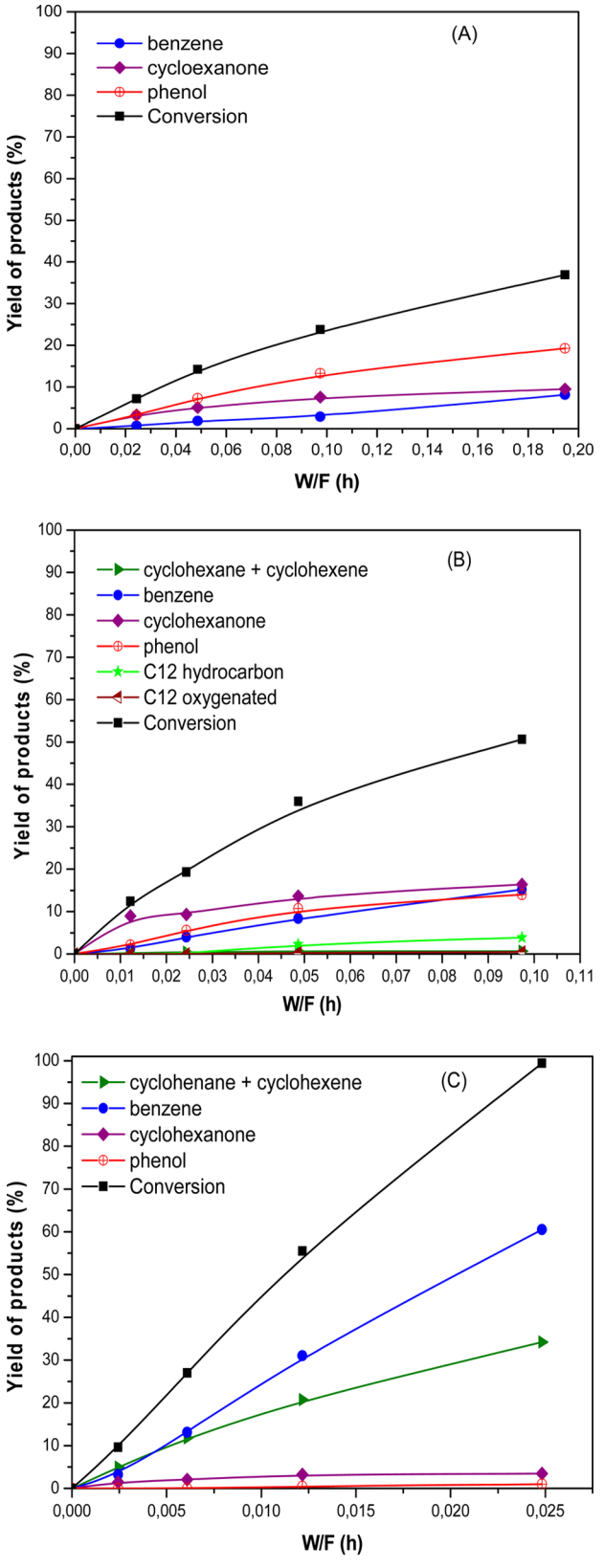

Figure 4. Cyclohexanol conversion and yield of products as a function of W/F over (A) Pd/SiO_2, (B) Pd/ZrO_2-N, and (C) Pd/Al_2O_3. Reaction conditions: T = 573 K, P = 1 atm, and H_2/cyclohexanol molar ratio 60.

highest W/F used when feeding phenol over the supported Pd catalysts. For SiO_2 and ZrO_2 supports, the conversion of cyclohexanol was very low, indicating that the contribution of dehydration catalyzed solely by the support is negligible. On the other hand, Al_2O_3 support exhibited high activity for dehydration of cyclohexanol, producing mainly cyclohexene. As a consequence, the formation of benzene by this reaction pathway over Al_2O_3 support cannot be ruled out.

The conversion of cyclohexanone over all catalysts yielded predominantly phenol as the main product formed. Only small amounts of cyclohexanol and benzene were detected over Pd/ZrO_2-N. Since phenol is the major product, it is likely that most of the benzene observed is produced as a secondary product from the direct conversion of phenol. In addition, bicyclic hydrocarbons such as biphenyl, 2-phenylphenol, cyclohexylbenzene, 2-cyclohexylcyclohexan-1-one, and 2-cyclohexylphenol were also obtained over the Al_2O_3- and ZrO_2-supported catalysts. Similar products have been observed during the conversion of cyclohexanone over Pt/Al_2O_3 catalysts.[42] Bicyclic products most probably arise from the alkylation of phenolic and aromatic rings by saturated alcohols, such as cyclohexanol and cyclohexanone.[43,24] Alkylation is catalyzed by acid sites such as Lewis acid sites present on the supports.

3.4. DRIFTS Experiments of HDO of Phenol, 2-Cyclohexen-1-one, Cyclohexanone, and Cyclohexanol over Pd/SiO_2, Pd/ZrO_2, and Pd/Al_2O_3 Catalysts. Figure 5 shows the DRIFTS spectra obtained upon exposure of the Pd/Al_2O_3 catalyst to a phenol/H_2 mixture at different temperatures. The spectrum at 373 K exhibits bands at 1289, 1495, 1595, 1687, 2857, 2942, 3034, and 3065 cm^{-1}. Table 4 gives the infrared vibrational wavenumbers and corresponding mode assignments for the adsorption of phenol on different materials on the basis of previous spectroscopic studies of phenol adsorption over oxides.[44−49]

The bands observed at 373 K at around 1289, 1495, 1595, 3034, and 3065 cm^{-1} correspond to the different vibrational modes of phenoxy species in either the monodentate or bidentate mode, which were formed by dissociative adsorption of phenol over the metal oxide cation (Lewis acid site). The band at 1289 cm^{-1} is assigned to the $\nu(CO)_{mono}$ stretching mode of phenoxy species. The bands at 1495 and 1595 cm^{-1} are due to the vibrations of the aromatic ring $\nu(C{=}C_{ring})$, whereas the bands at 3034 and 3065 cm^{-1} correspond to the $\nu(C{-}H)$ stretching mode of the aromatic ring of phenol. However, the bands at 2942, 2857, and 1687 cm^{-1} are not characteristic of adsorbed phenol, indicating the presence of other species. The bands in the range 2990−2850 cm^{-1} are typical of the $\nu(C{-}H)$ stretching mode of cyclohexane rings of cyclohexanol as well as cyclohexanone.[50] However, the DRIFTS spectrum of cyclohexanol exhibits bands at 1450, 1370, and 1050 cm^{-1} that are not present in the spectrum of Figure 5a. Furthermore, the typical band corresponding to the $\nu(C{=}O)$ stretching mode of carbonyl groups that appears at around 1715 cm^{-1} is not observed. Therefore, the spectrum of Figure 5a cannot be attributed to either cyclohexanol or cyclohexanone. In fact, the band at 1687 cm^{-1} has been assigned in the literature to the presence of 2-cyclohexen-1-one.[51] The infrared spectrum of 2-cyclohexen-1-one adsorbed on the surface of Au showed bands at 3034, 2950, 2870, and 1686 cm^{-1}, which are quite similar to those observed in this work. In fact, the shift of the band characteristic of the $\nu(C{=}O)$ stretching mode of carbonyl groups from 1715 to 1687 cm^{-1} is due to the conjugation between the carbonyl group and the double bond of the ring.[52]

DOI: 10.1021/cs501853t
ACS Catal. 2015, 5, 1318−1329

Table 3. Comparison of Performance of Pd/SiO_2, Pd/ZrO_2-N, and Pd/Al_2O_3 for Different Feeds

	catalyst								
	Pd/SiO_2			Pd/ZrO_2			Pd/Al_2O_3		
	phenol feed	ONE feed	OL feed	phenol feed	ONE feed	OL feed	phenol feed	ONE feed	OL feed
W/F (h)	0.160	0.024	0.194	0.049	0.049	0.048	0.160	0.138	0.006
conversion (%)	36.0	28.4	36.9	36.3	33.4	36.0	28.2	26.2	27.0
yield (%)									
ANE + ENE	0.1	0.0	0.0	0.1	0.0	0.7	0.1	1.5	11.8
benzene	10.5	0.3	8.1	20.5	2.1	8.4	6.6	3.3	13.1
ONE	23.7		9.5	13.8		13.7	17.5		2.1
OL	2.6	0.9		1.0	2.9		0.0	0.0	
phenol		27.2	19.3		14.5	10.7		12.4	0.0
C12	0.0	0.0	0.0	1.0	13.9	2.5	4.0	9.0	0.0

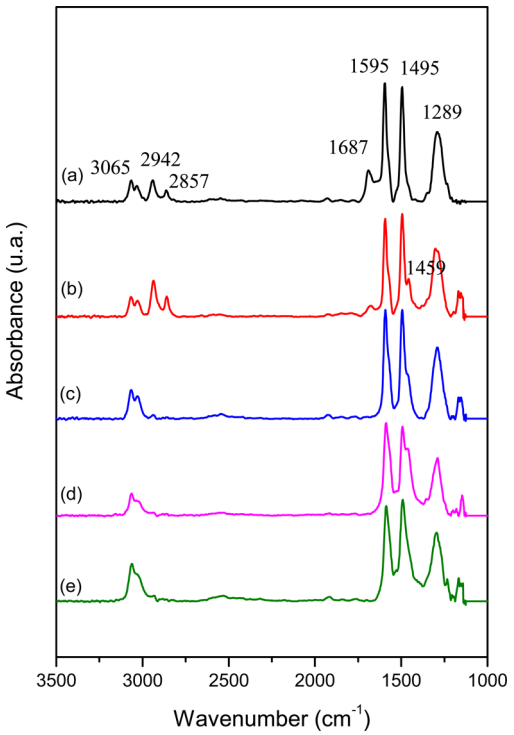

Figure 5. DRIFTS spectra obtained over Pd/Al_2O_3 catalyst under a reaction mixture containing phenol and hydrogen (H_2/phenol molar ratio 60) at different temperatures: (a) 373 K; (b) 473 K; (c) 573 K; (d) 673 K; (e) 773 K.

When the temperature was increased to 473 K, the intensity of the bands corresponding to phenoxy species (1289, 1495, 1595, 3030, 3068 cm^{-1}) and 2-cyclohexen-1-one species (1687 cm^{-1}) decreased. However, a new band appeared at 1459 cm^{-1} together with an increase in the intensity of the bands at 2937 and 2863 cm^{-1}. These results might indicate that phenoxy species are converted to cyclohexanol species.

When the temperature was further increased to 773 K, the intensity of the bands due to phenoxy and cyclohexanol species decreased, as they readily desorb from the surface.

In a second experiment, the Pd/Al_2O_3 catalyst was exposed to 2-cyclohexen-1-one (in He carrier) at 323 K and then a TPD was carried out in He. DRIFTS spectra are reported in Figure 6.

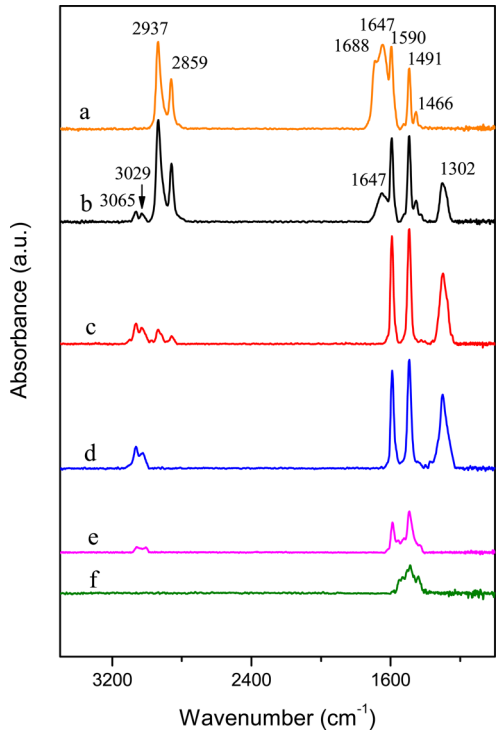

Figure 6. DRIFTS spectra obtained over Pd/Al_2O_3 catalyst for the TPD of 2-cyclohexen-1-one in flowing helium at different temperatures: (a) 323 K; (b) 373 K; (c) 473 K; (d) 573 K; (e) 673 K; (f) 773 K.

Table 4. Infrared Vibrational Wavenumbers and Mode Assignments for the Adsorption of Phenol on Different Catalysts

		vibrational wavenumber (cm^{-1})						
vibrational mode	adsorbed species	Al_2O_3[44,45]	ZrO_2[46]	MgO[46]	MnCe[47]	$CuCoFe_2O_4$[48]	CeO_2[49]	MgO[50]
$\nu(CH_{ring})$	phenoxy					3068; 3025		3075; 3040
$\nu(C{=}C_{ring})$	phenoxy	1597	1600	1600	1633	1587	1590	1590
$\nu(C{=}C_{ring})$	phenoxy	1498	1500	1500	1494	1485	1484	1490
$\nu(CO)_{mono}$	phenoxy	1295	1290	1300	1265	1255	1266	1300
$\nu(CO)_{bi}$	phenoxy	1250		1260			1242	

DOI: 10.1021/cs501853t
ACS Catal. 2015, 5, 1318−1329

The standard spectrum for gas-phase 2-cyclohexen-1-one (i.e., NIST database) displays the main bands at 2946, 2890−2846, 1710, 1438, and 1394−1382 cm^{-1}. For the Pd/Al_2O_3 catalyst, at 323 K, bands at 2937, 2859, and 1688 cm^{-1} are in good agreement with the standard, albeit shifted to lower wavenumbers due to adsorption onto the solid surface. However, additional bands are present. There is a band at 1647 cm^{-1} which is in good agreement with that expected for the adsorbed 2,4-cyclohexadien-1-one tautomer of phenol. When the temperature is increased to 373 K, the band at 1688 cm^{-1} for 2-cyclohexen-1-one has diminished, and the primary ν(C═O) stretching mode that remains corresponds to the tautomer. The bands corresponding to vibrational modes in the range of 2800−2950 cm^{-1} associated with C−H bonding do not change significantly in position, as the ring remains, for the most part, partially dehydrogenated (i.e., the diene has formed). However, low-intensity bands at 3065, 3029, and 1302 cm^{-1} demonstrate that phenol is also present. It is well-known that the keto/enol equilibrium for phenol is different from that for most systems, because the aromatic ring stabilizes the enol form.[53] Therefore, with increasing temperature, the phenol tautomer should dominate. When the temperature is increased to 473 K and again to 573 K, this is precisely what occurs, and the bands at 3065, 3029, 1590, and 1491 cm^{-1} for adsorbed phenol dominate the spectra (compare with Table 4 assignments). At higher temperatures, the coverage decreases.

The Pd/Al_2O_3 catalyst was also exposed to a cyclohexanone/H_2 mixture at different temperatures. The respective DRIFTS spectra are shown in Figure 7. At 373 K, bands at 2942, 2867, 1705, 1450, and 1355 cm^{-1} characteristic of cyclohexanone are observed.[50,51] Increasing the temperature to 473 K led to the disappearance of the band at 1705 cm^{-1} typical of the ν(C═O) stretching mode of the carbonyl group of cyclohexanone. However, the bands at 2942, 2867, and 1450 cm^{-1} remain unchanged, indicating that under these conditions cyclohexanone was converted to cyclohexanol. Heating to 573 K caused significant changes in the spectrum. The bands at 2942, 2867, and 1449 cm^{-1} diminished completely and new ones appeared at 3060, 3029, 1598, 1493, and 1293 cm^{-1}. As previously discussed, these bands correspond to adsorbed phenoxy species. Again, a further increase in temperature to 773 K decreased the intensity of the bands of phenoxy species.

Finally, Figure 8 displays the DRIFTS spectra of the cyclohexanol/H_2 mixture at different temperatures over Pd/Al_2O_3 catalyst. The spectrum at 373 K shows bands at 2934, 2858, 1451, and 1364 cm^{-1} characteristic of cyclohexanol. A band of weak intensity at 1697 cm^{-1} is also observed, indicating the formation of cyclohexanone. Increasing the temperature to 473 K decreased the intensity of the bands assigned to cyclohexanol, and the band attributed to cyclohexanone was no longer detected. When the catalyst was heated to 573 K, the bands typical of cyclohexanol disappeared, whereas new bands attributed to phenoxy species (3063, 3026, 1589, 1493, 1298 cm^{-1}) were observed. Increasing the temperature to 773 K decreased the intensity of the bands corresponding to phenoxy species.

A direct comparison was made by repeating the DRIFTS experiment with the phenol/H_2 mixture over the Pd/ZrO_2 catalyst at different temperatures. As shown in Figure 9, the spectra are much more complex than those observed for the Pd/Al_2O_3 catalyst. The DRIFTS spectra at 373 K displays bands at 2931, 2851, 2010, 1560, 1450, 1340, 1260, and 1049

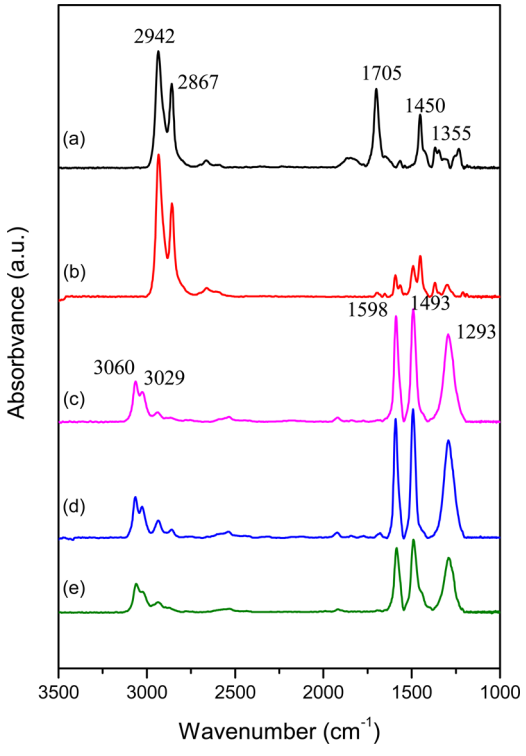

Figure 7. DRIFTS spectra obtained over Pd/Al_2O_3 catalyst in a reaction mixture containing cyclohexanone and hydrogen (H_2/cyclohexanone molar ratio 60) at different temperatures: (a) 373 K; (b) 473 K; (c) 573 K; (d) 673 K; (e) 773 K.

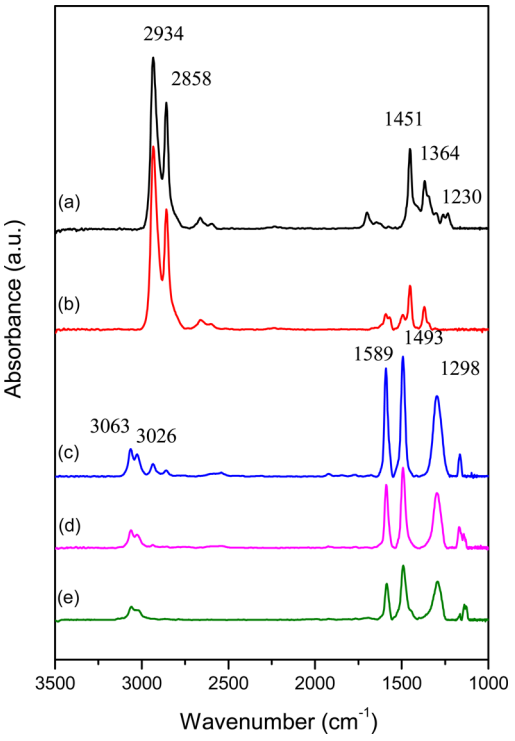

Figure 8. DRIFTS spectra obtained over Pd/Al_2O_3 catalyst in a reaction mixture containing cyclohexanol and hydrogen (H_2/cyclohexanol molar ratio 60) at different temperatures: (a) 373 K; (b) 473 K; (c) 573 K; (d) 673 K; (e) 773 K.

DOI: 10.1021/cs501853t
ACS Catal. 2015, 5, 1318−1329

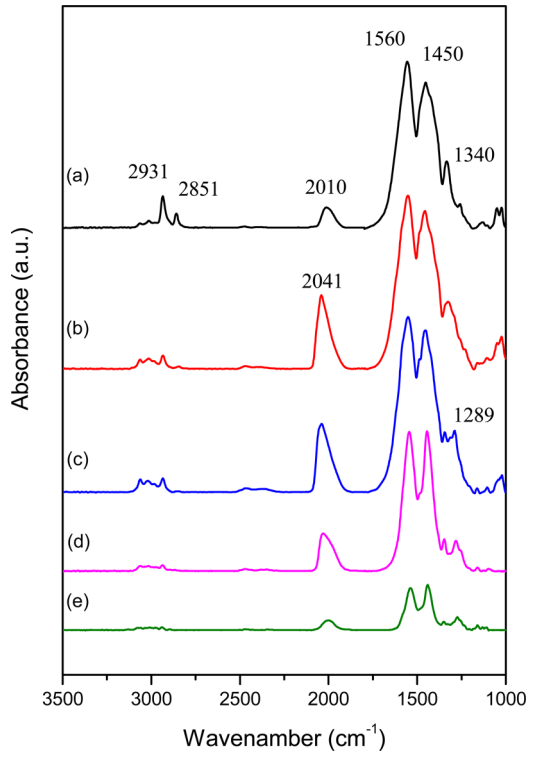

Figure 9. DRIFTS spectra obtained over Pd/ZrO_2 catalyst in a reaction mixture containing phenol and hydrogen (H_2/phenol molar ratio 60) at different temperatures: (a) 373 K; (b) 473 K; (c) 573 K; (d) 673 K; (e) 773 K.

cm^{-1} and a shoulder at 1482 cm^{-1}. In this case, the bands characteristic of phenoxy species were not detected. On the other hand, the bands at 2931, 2851, 1450, and 1049 cm^{-1} indicate that phenol adsorbs and reacts immediately, producing cyclohexanol. However, the bands at 1560, 1482, and 1340 cm^{-1} suggest the presence of other species. The band at 1560 cm^{-1} is shifted to lower wavenumbers from the bands characteristic of the vibrations of the aromatic ring (ν(C=C_{ring})). Therefore, these bands could be tentatively attributed to the ν(OCO) stretching mode of a phenol molecule adsorbed on the support, similar to the formation of carboxylate species by the adsorption of an alcohol such as ethanol.[54] In that case, the carbonyl interlocks with the defect site of the zirconia (e.g., at the Pd−zirconia interface), such that the bonding occurs at reduced Zr defect sites (e.g., oxygen vacancies or defect-associated type II bridging OH groups, with H_2O being formed once bonding has taken place). Note that the two types of defect sites are equivalent in the oxidation state of Zr (e.g., Zr^{3+} formalism). In this case, carbon is proposed to be bonded to both the oxygen originating from the phenoxy molecule and to that of the support adjacent to the defect, resulting in the observed band corresponding to the ν(OCO) vibration. The band at 2010 cm^{-1} indicates the presence of Pd−carbonyl species, most likely formed from the reaction of Pd with CO produced from the decomposition of residual carbonate (always present on metal oxide catalysts even after reduction).[55] Increasing the temperature to 573 K led to an increase in the intensity of the bands corresponding to the phenol molecule adsorbed at defect sites as well as the band at 2040 cm^{-1}. In addition, the bands assigned to cyclohexanol disappeared. A further increase in temperature to 773 K significantly decreased the intensity of all bands in the spectrum. The result emphasizes the catalytic action that is occurring. Since the reduced defect sites are proposed to be at the metal−support interface, the structure predisposes the molecule to attack by hydrogenation of the carbonyl bond from dissociated hydrogen (e.g., spillover from Pd). The subsequent dehydration of the resulting 2,4-cyclohexanol species results in a higher selectivity to benzene.

3.5. Proposed Pathway Reaction for Hydrodeoxygenation of Phenol. Two different reaction pathways have been typically proposed in the literature for the HDO of phenol: (i) the direct deoxygenation (DDO) that involves the cleavage of the C(sp^2)−O bond by hydrogenolysis and (ii) sequential hydrogenation (HYD) of the aromatic ring on metal sites

Scheme 1. HDO Reaction Pathways over Pd-Supported Catalysts

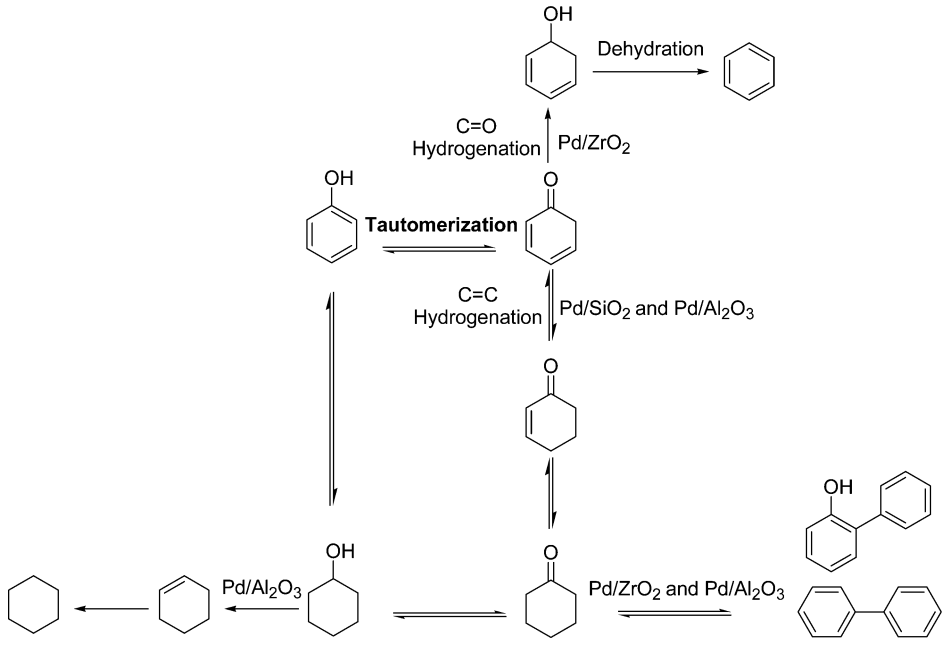

DOI: 10.1021/cs501853t
ACS Catal. 2015, 5, 1318−1329

Table 5. Product Distribution for HDO of Phenol at 573 K and Atmospheric Pressure over Ni-Based Catalysts

		selectivity (%)					
	conversion (%)	methane	benzene	ONE	OL	C_{12}	C_5–C_6
Ni/SiO_2	14.7	7.2	4.8	63.3	20.0	1.2	3.2
Ni/ZrO_2	11.4	15.4	26.7	37.7	10.9	5.4	6.4

followed by dehydration of cyclohexanol on acid sites.[56−59] However, the dissociation energy of the C−O bond of the aromatic ring is high and, therefore, it is unlikely that this reaction pathway occurs under typical reaction conditions.[60] It has been suggested that saturation of the aromatic ring is necessary to lower the energy barrier for breaking the C−O bond.[34,61] On catalysts containing sufficient acidity, this step occurs via dehydration.[32,43] In the present work, this could be the case for the Pd/Al_2O_3 catalyst. However, for Pd/SiO_2 and Pd/ZrO_2 catalysts, this reaction pathway is much less likely, since both supports do not have significant acidity, as shown by the DRIFTS of pyridine and the catalytic tests with the pure supports. Therefore, benzene should be formed by an alternative route. A similar result was reported for HDO of *m*-cresol over bulk Fe_2O_3 and Pd/Fe_2O_3 catalysts. In this case, it was noticed a high selectivity toward toluene production over the reduced Fe surface for the *m*-cresol HDO reaction in the case of unsupported Fe.[62]

Our DRIFTS experiments under reaction conditions over Pd/Al_2O_3 catalyst revealed the formation of 2-cyclohexen-1-one. This compound has also been reported in trace amounts during cyclohexanone conversion over Pt/Al_2O_3 catalysts.[42] Musselwhite et al. studied the kinetics of the hydrogenation of 2-cyclohexen-1-one over Pd/Al_2O_3 catalysts in the liquid phase.[63] They proposed that 2-cyclohexen-1-one is first hydrogenated to cyclohexanone and further hydrogenated to cyclohexanol. Therefore, the formation of this intermediate during the conversion of phenol should involve a tautomerization step, with the formation of a cyclohexadienone intermediate. This intermediate is highly unstable and could react by two different routes (Scheme 1). (i) Hydrogenation of the ring occurs, producing 2-cyclohexen-1-one, which is hydrogenated to cyclohexanone and then cyclohexanol. This is the typical reaction pathway for the HDO of phenol proposed in the literature (except for the 2-cyclohexen-1-one intermediate).[34] (ii) Hydrogenation of the carbonyl group occurs, leading to the formation of 2,4-cyclohexadienol, which is in turn dehydrated to benzene. The ratio of benzene to cyclohexane under our reaction conditions is higher than the equilibrium value. Therefore, benzene cannot come from cyclohexane via dehydrogenation. It would never exceed the equilibrium. In contrast, if benzene is formed first, then the ratio can be higher than the equilibrium value. In this case, cyclohexane may be formed via hydrogenation.

Recently, we have proposed a very similar mechanism for the HDO of *m*-cresol over Pd/SiO_2 and Pd/ZrO_2 catalysts.[18] In this case, *m*-cresol is tautomerized to the ketone form (3-methyl-3,5-cyclohexadienone). For Pd/SiO_2 catalyst, hydrogenation of the aromatic ring is favored, leading to 3-methylcyclohexanone and 3-methylcyclohexanol. On the other hand, hydrogenation of the carbonyl group, leading to the formation of 3-methyl-3,5-cyclohexadienol and then to toluene, is promoted over Pd/ZrO_2 catalyst. The differences in the reaction pathway were attributed to the presence of oxophilic sites. In the case of Pd/ZrO_2, the oxophilic sites are represented by incompletely coordinated Zr^{4+} cations (Lewis acid sites) near the perimeter of the metal particles. These oxophilic sites favor the interaction of the oxygen of the carbonyl group in the *m*-cresol tautomer intermediate with the catalyst surface. Then, the carbonyl group is preferentially hydrogenated on the metal particles at the metal−support interface, leading to the formation of toluene after the facile dehydration of the reactive intermediate.

In the present work, the same behavior was observed for the HDO of the phenol reaction. The higher selectivity to benzene for Pd/ZrO_2 in comparison to that for Pd/SiO_2 catalyst suggests that the oxophilic sites on the ZrO_2 support promote the deoxygenation activity by enhancing the hydrogenation of the C═O bond of the phenol tautomer formed. In addition, the C_{12} hydrocarbons observed in the case of Pd/ZrO_2 catalysts can be ascribed to an alkylation reaction of aromatic rings by saturated alcohols catalyzed by Lewis acid sites. For Pd/Al_2O_3 catalyst, the dehydration of cyclohexanol cannot be ruled out, due to the high acidity of the support.

The importance of the oxophilic sites on the ZrO_2 support for improving the deoxygenation activity of the HDO of the phenol reaction is also observed for other metals. The HDO reaction was performed over Ni/SiO_2 and Ni/ZrO_2 catalysts (5 wt % Ni) under the same reaction conditions used for Pd-based catalysts, and the results are reported in Table 5. For zirconia-supported catalysts, the selectivity to benzene is much higher than that observed with Pd/SiO_2 and Ni/SiO_2 catalysts. In addition, the selectivity to benzene was basically the same on Pd/ZrO_2 and Ni/ZrO_2 catalysts. The main difference between both catalysts was the higher selectivity to methane and C_5–C_6 hydrocarbons observed for the Ni/ZrO_2 catalyst. This is likely due to the higher hydrogenolysis activity of Ni.

4. CONCLUSIONS

Pd catalysts supported on SiO_2, Al_2O_3, and ZrO_2 were tested in the HDO reaction of phenol. The product distributions showed a remarkable dependence on the support used. Over Pd/SiO_2 and Pd/Al_2O_3 catalysts, the formation of cyclohexanone was favored, whereas benzene was promoted over Pd/ZrO_2 catalyst.

DRIFTS experiments revealed that a possible pathway is phenol tautomerization to a 2,4-cyclohexadienone intermediate. For Pd/SiO_2 and Pd/Al_2O_3 catalysts, the ring is preferentially hydrogenated to produce cyclohexanone and cyclohexanol. On the other hand, the intermediate is, to a greater extent, hydrogenated at the carbonyl function to yield 2,4-cyclohexadienol, which is subsequently dehydrated to benzene over Pd/ZrO_2. The differences in the reaction pathway were attributed to the presence of oxophilic sites on the ZrO_2 surface (Zr^{4+} cations).

■ ASSOCIATED CONTENT

Supporting Information

The following file is available free of charge on the ACS Publications website at DOI: 10.1021/cs501853t.

XRD patterns of Pd/SiO_2, Pd/ZrO_2-N, and Pd/Al_2O_3 (PDF)

DOI: 10.1021/cs501853t
ACS Catal. 2015, 5, 1318−1329

AUTHOR INFORMATION

Corresponding Author

*E-mail for F.B.N.: fabio.bellot@int.gov.br.

Notes

The authors declare no competing financial interest.

ACKNOWLEDGMENTS

Support from the National Science Foundation (EPSCoR0814361), the U.S. Department of Energy (DE-FG36GO88064), the Oklahoma Secretary of Energy, and the Oklahoma Bioenergy Center are greatly appreciated. Allocation of computing time provided by the OU Supercomputing Center for Education and Research (OSCER) at the University of Oklahoma is acknowledged. P.M.d.S. and R.C.R.-N. thank CAPES and FAPERJ for scholarships received. UK-CAER work was supported by the Commonwealth of Kentucky.

REFERENCES

(1) Wawrzetz, A.; Peng, B.; Hrabar, A.; Jentys, A.; Lemonidou, A. A.; Lercher, J. A. *J. Catal.* **2010**, *269*, 411−420.
(2) Chen, L.; Zhu, Y.; Zheng, H.; Zhang, C.; Zhang, B.; Li, Y. *J. Mol. Catal. A: Chem.* **2011**, *351*, 217−227.
(3) Faba, L.; Díaz, E.; Ordóñez, S. *Appl. Catal., B* **2014**, *160−161*, 436−444.
(4) McManus, J. R.; Vohs, J. M. *Surf. Sci.* **2014**, *630*, 16−21.
(5) Huber, G. W.; Chheda, J. N.; Barrett, C. J.; Dumesic, J. A. *Science* **2005**, *308*, 1446−1450.
(6) Barrett, C. J.; Cheda, J. N.; Huber, G. W.; Dumesic, J. A. *Appl. Catal., B* **2006**, *66*, 111−118.
(7) Hong, Y.-K.; Leea, D.-W.; Eoma, H.-J.; Lee, K.-Y. *J.Mol. Catal. A: Chem.* **2014**, *392*, 241−246.
(8) Moon, J.-S.; Kim, E.-G.; Lee, Y.-K. *J. Catal.* **2014**, *311*, 144−152.
(9) Zhang, X.; Zhang, Q.; Chen, L.; Xu, Y.; Wang, T.; Ma, L. *Chin. J. Catal.* **2014**, *35*, 302−309.
(10) Lee, C. R.; Yoon, J. S.; Suh, Y.-W.; Choi, J.-W.; Ha, J.-M.; Suh, D. J.; Park, Y.-K. *Catal. Commun.* **2012**, *17*, 54−58.
(11) Sitthisa, S.; Resasco, D. E. *Catal. Lett.* **2011**, *141*, 784−791.
(12) Güvenatam, B.; Kursuṇ, O.; Heeres, E. H. J; Pidkoa, E. A.; Hensen, E. J. M. *Catal. Today* **2014**, *233*, 83−91.
(13) Omotoso, T.; Boonyasuwat, B.; Crossley, S. P. *Green Chem.* **2014**, *16*, 645−652.
(14) Jin, S.; Xiao, Z.; Li, C.; Chena, X.; Wanga, L.; Xinga, J.; Li, W.; Liang, C. *Catal. Today* **2014**, *234*, 125−132.
(15) Elliot, D. C. *Energy Fuels* **2007**, *21*, 1792−1815.
(16) Furimsky, E. *Appl. Catal., A* **1998**, *171*, 177−206.
(17) Mochizuki, T.; Chen, S.-Y.; Toba, M.; Yoshimura, Y. *Appl. Catal., B* **2014**, *146*, 237−243.
(18) de Souza, P. M.; Nie, L.; Borges, L. E.; Noronha, F. B.; Resasco, D. E. *Catal. Lett.* **2014**, *144*, 2005−2011.
(19) Wang, W.; Yang, Y.; Bao, J.; Luo, H. *Catal. Commun.* **2009**, *11*, 100−105.
(20) Zhao, C.; HE, J.; Lemonidou, A. A.; Li, X.; Lercher, J. A. *J. Catal.* **2011**, *280*, 8−16.
(21) Zhang, X.; Wang, T.; Ma, L.; Zhang, Q.; Huang, X.; Yu, Y. *Appl. Energy* **2013**, *112*, 533−538.
(22) Echeandia, S.; Pawelec, B.; Barrio, V. L.; Arias, P. L.; Cambra, J. F.; Loricera, C. V.; Fierro, J. L. G. *Fuel* **2014**, *117*, 1061−1073.
(23) Guvenatam, B.; Kursun, O.; Heeres, E. H. J.; Pidko, E. A.; Hensen, E. J. M. *Catal. Today* **2013**, *233*, 83−91.
(24) Hong, D. Y.; Miller, S. J.; Agarwal, P. K.; Jones, C. W. *Chem. Commun.* **2010**, *46*, 1039−1040.
(25) Horacek, J.; Šťávová, G.; Kelbichová, V.; Kubicka, D. *Catal. Today* **2013**, *204*, 38−45.
(26) Matos, J.; Corma, A. *Appl. Catal., A* **2011**, *404*, 103−112.
(27) Mortensen, P. M.; Grunwaldt, J. D.; Jensen, P. A.; Knudsen, K. G.; Jensen, A. D. *Appl. Catal., B* **2011**, *407*, 1−19.
(28) Newman, C.; Zhou, X.; Goundie, B.; Ghampson, I. T.; Pollock, R. A.; Ross, Z.; Wheeler, M. C.; Meulenberg, R.; Austin, R. N.; Frederick, B. G. *Appl. Catal., A* **2014**, *477*, 64−74.
(29) Talukdar, A. K.; Bhattacharyya, K. G. *Appl. Catal., A* **1993**, *96*, 229−239.
(30) Shin, E. J.; Keane, M. A. *Ind. Eng. Chem. Res.* **2000**, *39*, 883−892.
(31) Zhao, C.; He, J.; Lemonidou, A. A.; Li, X.; Lercher, J. *J. Catal.* **2011**, *280*, 8−16.
(32) Zhao, C.; Kasakov, S.; He, J.; Lercher, J. *J. Catal.* **2012**, *296*, 12−23.
(33) Zhao, C.; Kou, Y.; Lemonidou, A. A.; Li, X.; Lercher, J. *Angew. Chem.* **2009**, *121*, 4047−4050.
(34) Mortensen, P. M.; Grunwaldt, J.-D.; Jensen, P. A.; Jensen, A. D. *ACS Catal.* **2013**, *3*, 1774−1785.
(35) Nie, L.; de Souza, P. M.; Noronha, F. B.; An, W.; Sooknoi, T.; Resasco, D. E. *J. Mol. Catal. A: Chem.* **2014**, *388−389*, 47−55.
(36) Nie, L.; Resasco, D. E. *J. Catal.* **2014**, *317*, 22−29.
(37) Zhu, X.; Nie, L.; Lobban, L. L.; Mallinson, R. G.; Resasco, D. E. *Energy Fuels* **2014**, *28*, 4104−4111.
(38) Resasco, D. E.; Crossley, S. P. *Catal. Today* **2014**, DOI: 10.1016/j.cattod.2014.06.037.
(39) Srinivasan, R.; Hubbard, C. R.; Cavin, O. B.; Davis, B. H. *Chem. Mater.* **1993**, *5*, 27−31.
(40) Nakano, Y.; Iizuka, T.; HaTorri, H.; Tanabe, K. *J. Catal.* **1979**, *57*, 1−10.
(41) Ouyang, F.; Nakayama, A.; Tabada, K.; Suzuki, E. *J. Phys. Chem. B* **2000**, *104*, 2012−2018.
(42) Nimmanwudipong, T.; Runnebaum, R. C.; Tay, K.; Block, D. E.; Gates, B. C. *Catal. Lett.* **2011**, *141*, 1072−1078.
(43) Zhao, C.; Camaioni, D. M.; Lercher, J. A. *J. Catal.* **2012**, *288*, 92−103.
(44) Popov, A.; Kondratieva, E.; Goupil, J. M.; Mariey, L.; Bazin, P.; Gilson, J.-P.; Travert, A.; Maugé, F. *J. Phys. Chem. C* **2010**, *114*, 15661−15670.
(45) Popov, A.; Kondratieva, E.; Gilson, J.-P.; Mariey, L.; Travert, A.; Maugé, F. *Catal. Today* **2011**, *172*, 132−135.
(46) Xu, B.-Q.; Yamaguchi, T.; Tanabe, K. *Mater. Chem. Phys.* **1988**, *19*, 291−297.
(47) D'alessandro, O.; Thomas, H. J.; Sambeth, J. E. *React. Kinet. Mech. Catal.* **2012**, *107*, 295−309.
(48) Mathew, T.; Vijayaraj, M.; Pai, S.; Tope, B. B.; Hegde, S. G.; Rao, B. S.; Gopinath, C. S. *J. Catal.* **2004**, *227*, 175−185.
(49) Mariey, L.; Lamotte, J.; Lavalley, J. C.; Tsyganenko, N. M.; Tsyganenko, A. A. *Catal. Lett.* **1996**, *41*, 209−211.
(50) Fridman, V. Z.; Davydov, A. A.; Titievsky, K. *J. Catal.* **2004**, *222*, 545−557.
(51) Liu, X.; Friend, C. M. *Langmuir* **2010**, *26*, 16552−16557.
(52) Silverstein, R. M. In *Spectrometric Identification of Organic Compounds*, 7th ed.; Webster, F. X., Kiemle, D., Eds.; Wiley: Hoboken, NJ, 2005; p 62.
(53) Gadosy, T. A.; McClelland, R. A. *J. Mol. Struct. (THEOCHEM)* **1996**, *369*, 1−8.
(54) Mattos, L. V.; Jacobs, G.; Davis, B. H.; Noronha, F. B. *Chem. Rev.* **2012**, *112*, 4094−4123.
(55) Pigos, J. M.; Brooks, C. J.; Jacobs, G.; Davis, B. H. *Appl. Catal., A* **2007**, *319*, 47−57.
(56) Wan, H.; Chaudhari, R. V.; Subramaniam, B. *Top. Catal.* **2012**, *55*, 129−139.
(57) Gevert, B. S.; Otterstedt, J. E.; Massoth, F. E. *Appl. Catal.* **1987**, *1*, 119−131.
(58) Furimsky, E.; Mikhlin, J. A.; Jones, D. Q.; Adley, T.; Baikowitz, H. *Can. J. Chem. Eng.* **1986**, *6*, 982−985.
(59) Romero, Y.; Richard, F.; Brunet, S. *Appl. Catal., B* **2010**, *98*, 213−223.
(60) Furimsky, E. *Appl. Catal., A* **2000**, *199*, 147−190.
(61) Benson, S. W. *Thermochemical Kinetics: Methods for Estimation of Thermochemical Data and Rate Parameters*, 2nd ed.; Wiley: New York, 1976.

DOI: 10.1021/cs501853t
ACS Catal. 2015, 5, 1318−1329

(62) Hong, Y.; Zhang, H.; Sun, J.; Ayman, K. M.; Hensley, A. J. R.; Gu, M.; Engelhard, M. H.; Mc Ewen, J. S.; Wang, Y. *ACS Catal.* **2014**, *4*, 3335−3345.
(63) Musselwhite, N. E.; Wagner, S. B.; Manbeck, K. A.; Carl, L. M.; Gross, K. M.; Marsh, A. L. *Appl. Catal., A* **2011**, *402*, 104−109.

DOI: 10.1021/cs501853t
ACS Catal. 2015, 5, 1318−1329